Proc. Natl. Acad. Sci. USA
Vol. 92, pp. 3668–3672, April 1995
Biochemistry

Use of binding energy by an RNA enzyme for catalysis by positioning and substrate destabilization

GEETA J. NARLIKAR[*], VIDHYA GOPALAKRISHNAN[†], TIMOTHY S. MCCONNELL[§], NASSIM USMAN[¶], AND DANIEL HERSCHLAG[*†‖]

Departments of [†]Biochemistry and [*]Chemistry, Stanford University, Stanford, CA 94305; [§]Department of Chemistry and Biochemistry, University of Colorado, Boulder, CO 80309; and [¶]Ribozyme Pharmaceuticals Inc., 2950 Wilderness Place, Boulder, CO 80301

Communicated by William P. Jencks, Brandeis University, Waltham, MA, December 27, 1994

ABSTRACT A fundamental catalytic principle for protein enzymes is the use of binding interactions away from the site of chemical transformation for catalysis. We have compared the binding and reactivity of a series of oligonucleotide substrates and products of the *Tetrahymena* ribozyme, which catalyzes a site-specific phosphodiester cleavage reaction: CCCUCUpA + G ⇌ CCCUCU-OH + GpA. The results suggest that this RNA enzyme, like protein enzymes, can utilize binding interactions to achieve substantial catalysis via entropic fixation and substrate destabilization. The stronger binding of the all-ribose oligonucleotide product compared to an analog with a terminal 3′ deoxyribose residue gives an effective concentration of 2200 M for the 3′ hydroxyl group, a value approaching those obtained with protein enzymes and suggesting the presence of a structurally well defined active site capable of precise positioning. The stabilization from tertiary binding interactions is 40-fold less for the oligonucleotide substrate than the oligonucleotide product, despite the presence of the reactive phosphoryl group in the substrate. This destabilization is accounted for by a model in which tertiary interactions away from the site of bond cleavage position the electron-deficient 3′ bridging phosphoryl oxygen of the oligonucleotide substrate next to an electropositive Mg ion. As the phosphodiester bond breaks and this 3′ oxygen atom develops a negative charge in the transition state, the weak interaction of the substrate with Mg^{2+} becomes strong. These strategies of "substrate destabilization" and "transition state stabilization" provide estimated rate enhancements of ≈280- and ≈60-fold, respectively. Analogous substrate destabilization by a metal ion or hydrogen bond donor may be used more generally by RNA and protein enzymes catalyzing reactions of phosphate esters.

Since the discovery of catalytic RNA, the definition of an enzyme has been modified to include RNA enzymes or ribozymes (1–3). The ribozyme derived from the *Tetrahymena* self-splicing group I intron catalyzes a reaction analogous to the first step of splicing (Eq. 1). This ribozyme provides a rate enhancement of 10^{11}-fold over the uncatalyzed reaction, comparable to that observed for many protein enzymes (4).

```
CCCUCUpA(E·SA) + G → CCCUCU-OH(E·POH) + GpA
||||||               ||||||
┌AGGGAGG-5′          ┌AGGGAGG-5′                [1]
└─ E                 └─ E
```

Catalysis requires selective stabilization of a reaction's transition state without equivalent stabilization of the ground state. If the ground state and transition state were stabilized to the same extent by an enzyme, then the energetic barrier for reaction would remain unaltered and there would be no catalysis. A comprehensive analysis by Jencks (5) has indicated that protein enzymes use binding interactions with groups on the substrate not directly involved in the chemical transformation to achieve selective transition state stabilization.

Binding interactions between enzymes and their substrates can be used to precisely position substrates, thereby preferentially stabilizing the transition state by decreasing the entropic barrier for reaction (5). On one level, the *Tetrahymena* ribozyme is similar to protein enzymes as they both have specific binding sites for substrates. These binding sites use base-pairing and tertiary interactions to hold the oligonucleotide substrate and guanosine in place (6–13). However, the actual catalytic contribution of the binding interactions in an RNA enzyme depends on how precisely the substrates are fixed relative to one another. The results presented here suggest that the *Tetrahymena* ribozyme can use tertiary interactions to achieve significant entropic fixation of substrates, approaching that obtained by protein enzymes.

Protein enzymes can also achieve selective transition state stabilization by the strategy of "substrate destabilization." In this strategy, the enzyme uses binding interactions to juxtapose substrate and enzymic functional groups that would not otherwise interact in the ground state but that do interact strongly in the transition state (5). This strategy is now extended to an RNA enzyme. In addition, the specific mechanism for substrate destabilization suggested here for the *Tetrahymena* ribozyme may be used more generally by RNA and protein enzymes catalyzing cleavage of phosphate and carbon esters.

MATERIALS AND METHODS

Materials. L-21 *Sca* I ribozyme (E) was prepared by *in vitro* transcription as described (14). Oligonucleotides were prepared by solid-phase synthesis (15). For CCCUC 3′-dU (P_H), 3′-deoxyuridine (Sigma) was 5′-*O*-dimethoxytritylated and 2′-O-succinylated according to standard procedures and coupled to activated LCAA-CPG (acid pretreated) by a water-soluble carbodiimide (16). CCCUCUpMe (S_{Me}) was synthesized by using a methyl phosphoramidite (17) and deprotected under mild conditions (3:1, NH_4OH/EtOH, 20°C, 8 h).

Kinetic Measurements. All reactions were single turnover, with E in excess of 5′-end-labeled oligonucleotide at 50°C in 50 mM NaMes (pH 6.6) and 10 mM $MgCl_2$ as described (4, 10, 18).

K_a^E Values. K_a^E (Fig. 1) was obtained for S_A and S_{Me} from the ratio k_{on}/k_{off}, where k_{off} is the rate constant for dissociation of S_A or S_{Me} from E (obtained from pulse–chase experiments) and k_{on} is the rate constant for association of S_A or S_{Me} with E [obtained from $(k_{cat}/K_m)^S$] (4, 18). The ratio k_{on}/k_{off} equals K_a^E because the open complex (Fig. 1) does not accumulate under these reaction conditions. K_a^E values for P_{OH} and P_H were obtained from the dependence of the rate of miscleavage on E concentration (13, 19). The standard L-21 *Sca* I ribozyme (14) begins with the internal guide sequence (IGS) and has a

The publication costs of this article were defrayed in part by page charge payment. This article must therefore be hereby marked "*advertisement*" in accordance with 18 U.S.C. §1734 solely to indicate this fact.

Abbreviations: IGS, internal guide sequence of ribozyme; IGS′, oligonucleotide (GGAGGGA) having the same sequence as the ribozyme's IGS; LFER, linear free energy relationship.
‖To whom reprint requests should be addressed.

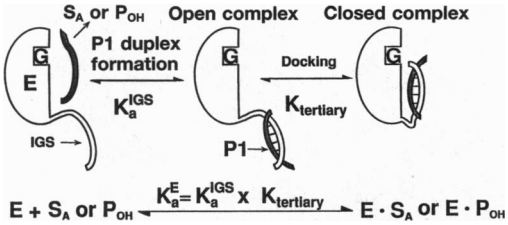

FIG. 1. Two-step binding of S_A or P_{OH} to the ribozyme. The oligonucleotide first forms the open complex by base pairing with the IGS of the ribozyme to give the P1 duplex (Eq. 1). The P1 duplex then docks into tertiary interactions with the ribozyme to form the closed complex (see Fig. 2) (7–13, 19, 20). K_a^E is the observed association constant for binding to the ribozyme (E), K_a^{IGS} is the association constant for binding in the open complex, and $K_{tertiary}$ is the equilibrium constant for docking into the tertiary interactions to form the closed complex.

triphosphate group attached to the G residue at the 5′ end of the IGS. K_a^E values were the same, whether E had a 5′ OH or a 5′ triphosphate, ruling out possible complications from the triphosphate.

K_a^{IGS} Values. Substrate inhibition was used to measure the stabilities of model P1 duplexes, where an oligonucleotide strand having the IGS sequence GGAGGGA (IGS′) or GGAGGG was used as an inhibitor of the ribozyme reaction (Eq. 2). Controls showing that the inhibition constant K_a^I represents the equilibrium constant $K_a^{IGS'}$ are described elsewhere (ref. 13; unpublished data).

$$IGS' \cdot S_A \underset{\pm IGS'}{\overset{K_a^I}{\rightleftharpoons}} E^G + S_A \overset{k_{cat}/K_m}{\rightleftharpoons} E + P_{OH} + GpA \qquad [2]$$

The duplex stability for P_{OH} was obtained analogously by following the reverse reaction in Eq. 2. The duplex stability of P_H was measured by following inhibition of its miscleavage.

A Linear Free Energy Relationship (LFER) Between Mg^{2+} Affinity and Effective Charge on an Oxygen Atom in Related Compounds. Bronsted LFERs are plots of the logarithm of a rate or equilibrium constant against pK_a values for a series of related compounds (XRO-H, with different X substituents). The slopes, referred to as β values, provide a measure of the change in effective charge in going from a ground state to a transition state (XRO-P $\rightarrow$ $[XRO^{\delta-} \cdots P]^{\ddagger}$; $\beta_{leaving\ group}$) or starting material to product (R′O-P + XRO-H $\rightleftharpoons$ R′OH + XRO-P; $\beta_{equilibrium}$) relative to the change in charge for the deprotonation equilibrium (XRO-H $\rightleftharpoons$ XRO^- + H^+) (21, 22). The deprotonation equilibrium is used as a standard such that the oxygen atom is defined as having effective charges of −1 and 0 in RO^- and ROH, respectively.

To construct the LFER, the relative Mg^{2+} affinities of ROH and RO^- were first estimated. The pK_a of $Mg(H_2O)_6^{2+}$ is 11.5 (23). A statistical correction for the 12 ionizable protons gives a pK_a' of 12.6. An analogous correction for the 2 ionizable protons of free water gives a pK_a' of 16.1. Mg^{2+} thus lowers the pK_a of water by 3.5 units (= 16.1 − 12.6). It is assumed that Mg^{2+} lowers the pK_a of an alcohol (RO-H), such as the 3′ hydroxyl of P_{OH}, by the same amount.** Therefore, the affinity of Mg^{2+} for RO^- (effective charge = −1 relative to 0 in RO-H) is ≈3200-fold ($10^{3.5}$) greater than for RO-H. The relative Mg^{2+} affinities of RO-H and RO^- and their effective charges of 0 and −1, respectively, then define a crude LFER represented by the line in Fig. 3*A*.

Next, the relative Mg^{2+} affinities of the bridging oxygen in the ground state (RO-P) and transition state ($[RO^{\delta-} \cdots P]^{\ddagger}$) for cleavage of a phosphate diester were estimated from this LFER by using the effective charges (β values) for RO-P and $[RO^{\delta-} \cdots P]^{\ddagger}$ (see Fig. 3*A*) relative to RO-H (β_{rel}). The effective charge for the bridging oxygen of a phosphate diester, XRO-P, is defined as +0.7 relative to XRO-H from the Bronsted $\beta_{equilibrium}$ value of +0.7; for the equilibrium, R′O-P + XRO-H $\rightleftharpoons$ R′OH + XRO-P (for a series of XRO-H species) (26). The value of $\beta_{leaving\ group}$ = −1.2 for the hydrolysis of a series of phosphate diesters; XRO-P $\rightarrow$ $[XRO^{\delta-} \cdots P]^{\ddagger}$ then relates the effective charge of the leaving group oxygen atom in the transition state, $[XRO^{\delta-} \cdots P]^{\ddagger}$, to that for this oxygen in the phosphate diester XRO-P (effective charge = +0.7 relative to XRO-H) (27). This gives an effective charge for the transition state of −0.5 [= +0.7 + (−1.2)] relative to XRO-H.

RESULTS AND DISCUSSION

We were initially intrigued by the paradoxical result that the oligonucleotide substrate S_{A5} binds ≈2-fold weaker to the ribozyme than the oligonucleotide product P_{OH} (Scheme I)

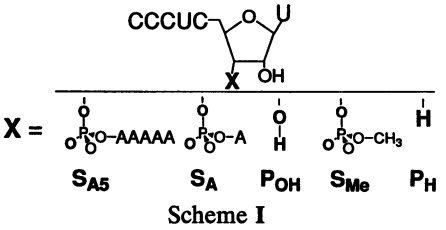

Scheme I

(4). This was surprising because S_{A5} contains the reactive phosphoryl group, which might be expected to make favorable interactions with the active site; indeed, substitution of the *pro*-S_P phosphoryl oxygen by a sulfur slows the cleavage by ≈10^3-fold (28, 29). First the trivial explanation that the non-base-paired dangling A tail was making unfavorable interactions in the active site was tested by comparing the binding affinity of S_A, which contains only a single A residue, to the binding of P_{OH} (Scheme I). S_A bound 8-fold weaker than P_{OH}, indicating that the longer A tail of S_{A5} was not responsible for the destabilizing effect (K_a^E; Table 1).

The oligonucleotide substrate and product bind to the ribozyme in two steps (Fig. 1) (19, 20). Since the first step involves P1 duplex formation with the IGS of E (Fig. 1), the 3′ dangling A residue of S_A (Eq. 1) was expected to strengthen

Table 1. Relative binding affinities of substrate and product analogs

Analog	K_a^E, × 10^6 M^{-1}	K_a^{IGS}, × 10^6 M^{-1}	K_{tert}	K_{tert}^{rel}
CCCUCU-OH (P_{OH})	420	0.7	600	1
CCCUCUpA (S_A)	50	3.1	16	1/40
CCCUCUpMe (S_{Me})	13	1.1	12	1/50
CCCUC 3′-dU (P_H)	13	0.9	14	1/40

Reactions were at 50°C in 50 mM NaMES, pH 6.6/10 mM $MgCl_2$. K_a^E values for S_A and S_{Me} varied by ±30% and values for P_{OH} and P_H varied by ±10% in independent experiments; $K_a^{IGS} = K_a^{IGS'}$, obtained from model P1 duplexes (Eq. 2; see text). Each $K_a^{IGS'}$ value was measured side by side with P_{OH}. Ratios varied by ±10% and each individual $K_a^{IGS'}$ value varied by ±20% in independent experiments; $K_{tert} = K_a^E/K_a^{IGS}$ (see Fig. 1); $K_{tert}^{rel} = K_{tert}^{analog}/K_{tert}^{POH}$. The estimated uncertainty in K_{tert}^{rel} values is ±20%.

**That HOH and ROH and their respective anions behave similarly with respect to Mg^{2+} affinity is suggested by the following: (*i*) The interaction of HOH and ROH and their respective anions with Mg^{2+} is predominantly electrostatic and the same change in charge of 1 from loss of a proton is obtained for both. (*ii*) Water and simple alcohols have similar pK_a values, ≈16 (24). (*iii*) The affinity of another metal ion, Fe^{3+}, for HOH and HO^- can be predicted from a LFER of affinities of Fe^{3+} for a series of substituted phenolates (25). See also †† and ¶¶ below.

binding rather than weaken it as observed, because 3′ overhanging residues contribute to RNA·RNA duplex stability (30). To further investigate the magnitude and origin of the observed destabilization, the energetic effects in the individual binding steps were separated.

Substrate inhibition was used to determine the stabilities of model P1 duplexes (see *Materials and Methods*). Several comparisons have strongly suggested that model duplexes with IGS′ have the same stability as the open complex on the ribozyme (Fig. 1) (refs. 13 and 20; unpublished data). Therefore, the stability of model P1 duplexes can be used as a measure of the stability of the open complex. The substrate S_A forms a 5-fold stronger P1 duplex than P_{OH} but binds 8-fold weaker overall (Table 1). The P1 duplex stability and the overall binding affinity give the tertiary stabilization on the ribozyme (Fig. 1). Tertiary interactions stabilize S_A 40-fold less than P_{OH} (Table 1). The destabilizing effect on the tertiary interactions is therefore larger than the observed overall difference in binding. An analogous result with a shortened substrate and product was recently reported (31).

A possible explanation for the observed destabilization of S_A was that the 3′ terminal A of S_A makes an unfavorable ground state interaction with the ribozyme, perhaps resulting in unstacking of this residue (4, 31, 32). To test this possibility, the tertiary binding energy of S_{Me} (Scheme **I**), which lacks the 3′ terminal A, was measured. S_{Me} binds ≈3-fold weaker to the ribozyme than S_A and also binds correspondingly weaker in the model P1 duplex (Table 1). Thus, the tertiary stabilization of S_{Me} is similar to that of S_A (Table 1), indicating that the weaker tertiary interactions of S_A were not due to unfavorable interactions with the 3′ terminal A. Furthermore, the rate of chemical cleavage for S_{Me} is only ≈3-fold slower than that for S_A, indicating that the 3′ terminal A does not contribute significantly to transition state stabilization (unpublished results). Thus, the A residue does not contribute significantly to catalysis or to destabilization of S_A and the origin of the observed destabilization is localized to the reactive phosphoryl group.

In S_{Me}, the reactive phosphoryl group is attached to the bridging oxygen, while in P_{OH}, a hydrogen atom is attached to this bridging oxygen (Scheme **I**). To investigate the role of this oxygen atom in the observed destabilization, the 3′ oxygen was removed altogether (P_H; Scheme **I**). P_H binds 30-fold weaker to the ribozyme than P_{OH} and forms a 1.4-fold weaker model P1 duplex than P_{OH} (Table 1). Thus, tertiary interactions stabilize P_H 40-fold less than P_{OH}, indicating that the 3′ OH of P_{OH} makes a strong interaction with the ribozyme.

Previous work has provided strong evidence for a direct interaction between an active site Mg^{2+} and the 3′ bridging oxygen of the reactive phosphoryl group in the transition state (33). Since the 3′ bridging oxygen atom develops a partial negative charge in the transition state as the phosphodiester bond breaks, this Mg^{2+} is expected to contribute to transition state stabilization (33, 34). The relative tertiary stabilities described here can all be explained by a model involving an interaction with this Mg ion, as presented below.

An interaction between the 3′ OH of P_{OH} and the Mg^{2+} explains the greater tertiary stabilization of P_{OH} relative to P_H. In the absence of additional interactions with P_{OH}, water would outcompete the 3′ OH of P_{OH} for this Mg^{2+} since there is much more water present (55 M) and since the electrostatic properties of an oxygen of an alcohol and water are similar.†† However, the 40-fold stronger binding of P_{OH} relative to P_H indicates a 40-fold preference of the Mg^{2+} for interacting with the 3′ OH than with 55 M water when P_H is bound. Thus, the 3′ OH has an effective concentration of 40 × 55 M = 2200 M relative to

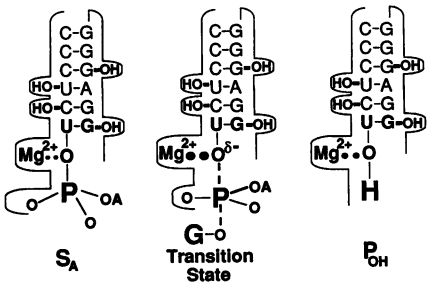

FIG. 2. Model for use of binding energy by the ribozyme for positioning and substrate destabilization. The G·U pair in boldface at the cleavage site and the 2′ hydroxyl groups explicitly shown make specific tertiary interactions with the ribozyme (7–13) that position the 3′ OH of P_{OH} (*Right*) adjacent to the active site Mg^{2+}; this results in the high effective concentration of the 3′ OH of 2200 M (see text). These tertiary interactions also position the electron-deficient bridging phosphoryl oxygen of the substrate next to the catalytic Mg^{2+}, inducing an electrostatic interaction not favored in solution. This "substrate destabilization" is indicated by small dots. In the transition state, the bridging oxygen develops a partial negative charge and interacts strongly with the Mg^{2+}, as indicated by large dots. The ribozyme is represented schematically by the thin outline. The ribozyme also presumably uses the intrinsic rigidity of an RNA·RNA duplex in positioning of the P1 duplex in the active site.

the OH of water (5). This value approaches the values of 10^4–10^5 M observed with protein enzymes (35–37).

The high effective concentration presumably reflects a combination of two phenomena: (*i*) tertiary interactions position the 3′ OH in the active site, thereby lowering the entropic barrier for binding to the active site Mg^{2+} relative to the entropic barrier for binding of a water molecule from solution (Eqs. **3a** and **3b**), and (*ii*) the ribozyme positions the 3′ hydrogen of P_H so that it interferes with the ability of water from solution to solvate the active site Mg^{2+} (Eq. **3c**).§§

$$E_{Mg}^{CH_2} + P\text{-}OH \xrightleftharpoons{K_{tertiary}} E_{Mg}^{CH_2\,P\text{-}OH} \xrightleftharpoons{40} E_{Mg}^{OH\,P_i} + H_2O\ (55\ M) \qquad [3a]$$

$$E_{Mg}^{CH_2} + P\text{-}H \xrightleftharpoons{K_{tertiary}} E_{Mg}^{CH_2\,P\text{-}H} \qquad [3b]$$

$$E_{Mg}^{CH_2} + P\text{-}H \xrightleftharpoons{K_{tertiary}} E_{Mg}^{H\,P_i\,CH_2} \qquad [3c]$$

Both require precise positioning in a structurally well-defined site because a floppy active site would not allow a high effective concentration via entropic fixation or interference with solvation.

The destabilization of S_A relative to P_{OH} is also predicted from an interaction with this active site Mg^{2+} because the phosphorylated 3′ oxygen of S_A is electron deficient relative to the protonated 3′ oxygen of P_{OH}, as suggested by the following data with model phosphate compounds: LFERs for equilibrium constants of model phosphodiesters indicate that the bridging phosphoryl oxygen behaves as though it has a positive charge of +0.7 relative to a protonated oxygen (26). P-O bonds are very stable and have bond lengths that are 10–20% shorter than those calculated for single σ bonds. The extra stability and shorter bond lengths have been proposed to arise due to donation of electrons from oxygen to phosphorus in a $p\pi$-$d\pi$ back-bond (38, 39), which would lead to a reduction in the charge density on the oxygen.

Thus, in solution, a positively charged Mg^{2+} would be predicted to interact preferentially with an oxygen from water

††As the pK_a of a nucleoside 3′ OH is somewhat lower than that for water or a simple alcohol such as ethanol (pK_a = 13 vs. 16), water is expected to have a small electrostatic advantage for interacting with Mg^{2+}. See also **.

§§The relative affinity of P_{OH} and P_H for the ribozyme is the same in 3–50 mM $MgCl_2$, suggesting that the Mg^{2+} adjacent to the 3′ oxygen remains bound even when the 3′ OH in P_{OH} is replaced by a 3′ H in P_H. The possibility exists that the 3′ O interacts with the Mg^{2+} in the transition state but not in the P_{OH} ground state, although there are no data that support this more complex alternative model.

(or an alcohol such as the 3′ OH of P_{OH})** rather than with an electron-deficient phosphorylated oxygen if both were present in equal concentrations. However, on the ribozyme, we propose that the electron-deficient phosphorylated oxygen of S_A is positioned adjacent to the Mg^{2+} by favorable tertiary interactions with the P1 duplex away from the site of bond cleavage (7–13). This results in a $Mg^{2+} \cdots$ (R)O-P interaction that is not favored in solution (Fig. 2). In other words, the tertiary interactions provide an entropic advantage to the 3′ bridging oxygen of S_A over water in solution. This overcomes the electrostatic advantage of the oxygen of water relative to the 3′ bridging oxygen for interacting with the Mg^{2+}.

In contrast to this destabilizing ground state interaction between the bridging phosphoryl oxygen atom of S_A and the active site Mg^{2+}, the interaction in the transition state is expected to be stabilizing because the partial negative charge on the bridge oxygen in the transition state results in a stronger electrostatic interaction relative to water (Fig. 2) (33, 34). The ribozyme-bound Mg^{2+} thus plays a catalytic role both by destabilizing the ground state ($E{\cdot}S_A$) and by stabilizing the transition state, relative to interaction of Mg^{2+} with water.

Physical organic data, which provide a rough quantitative estimate of the catalysis resulting from substrate destabilization and transition state stabilization, suggest a substantial contribution from both. Fig. 3*A* shows a correlation of Mg^{2+} affinity with the effective charges on oxygen. This correlation suggests that Mg^{2+} binds ≈16,000-fold tighter to the transition state for phosphodiester hydrolysis, $[RO^{\delta-} \cdots P]^{\ddagger}$, compared to the ground state, RO-P.¶¶ Of the total rate enhancement of ≈16,000-fold, ≈280-fold is estimated to arise from ground state destabilization relative to P_{OH} (RO-H) ($\Delta G_{destabilization}$) and ≈60-fold from transition state stabilization relative to P_{OH} ($\Delta G_{stabilization}$).

The substrate destabilization and transition state stabilization estimated above are depicted in the free energy reaction profile of Fig. 3*B*. Because free energies can be measured only relative to one another, a standard for comparison must be adopted in order to assign interactions as stabilizing or destabilizing. The energies in Fig. 3*B* are shown relative to P_{OH} because this species is expected to behave similar to water in its electrostatic interactions with Mg^{2+}.** Thus, the destabilization of S_A and the stabilization of the transition state in Fig. 3*B* represent the electrostatic effects relative to those with solvent. This seems to be an appropriate comparison as an enzyme is faced with the task of catalyzing a reaction relative to that in aqueous solution. If there were no positioning interactions, the bridging oxygen atom would not interact with the Mg^{2+} in the ground state and the maximum amount of electrostatic catalysis possible would be 60-fold, representing the stronger electrostatic interaction of Mg^{2+} with the transition state than with water ($\Delta G_{stabilization}$; Fig. 3*A*). Forcing a ground state interaction by fixing the bridging oxygen atom next to the Mg^{2+} would introduce substrate destabilization and increase the amount of catalysis from 60- to 1.6 × 10^4-fold.

CCCmUCUA (mU = 2′-methoxy, 2′-deoxyU), which is not stabilized by tertiary interactions in the ground state, is cleaved ≈50-fold slower than S_A, suggesting that tertiary interactions, which are proposed to position the substrate in the active site and induce substrate destabilization, do indeed contribute to lowering the barrier for the chemical step (refs. 10 and 13; unpublished data).

It is striking that the ≈280-fold weaker affinity of Mg^{2+} for RO-P than RO-H is within reasonable agreement with the

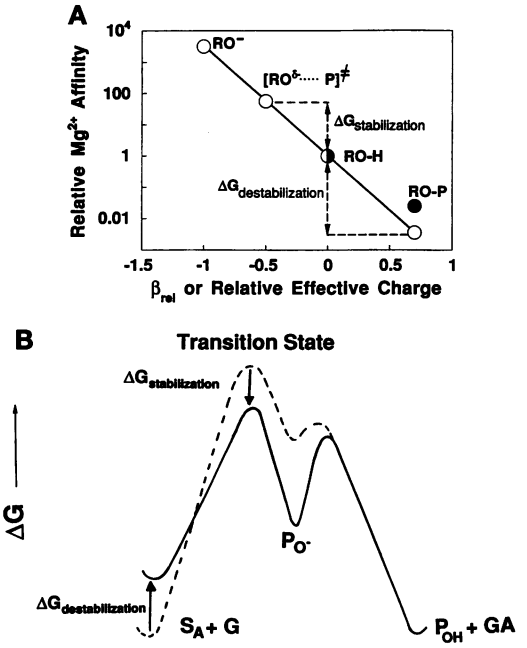

FIG. 3. Quantitative estimate of electrostatic catalysis caused by the active site Mg^{2+}. (*A*) Linear free energy correlation of Mg^{2+} affinities and effective charge on oxygen atoms of various species. Open symbols represent estimated Mg^{2+} affinities and effective charges for model compounds (see *Materials and Methods*); solid symbols represent relative stability of S_A (RO-P) and P_{OH} (RO-H) bound to the ribozyme. $\Delta G_{destabilization}$ = 3.6 kcal/mol (50°C) (1 cal = 4.184 J) corresponds to ≈280-fold destabilization of RO-P relative to R-OH and $\Delta G_{stabilization}$ = 2.6 kcal/mol corresponds to ≈60-fold stabilization of $[R\text{-}O^{\delta-} \cdots P]^{\ddagger}$ relative to ROH. (*B*) Free energy reaction profile showing proposed energetics from electrostatic interactions with the active site Mg^{2+} in the ribozyme reaction $E{\cdot}S_A + G \rightarrow E{\cdot}P_{OH} + GA$. Dashed line represents a hypothetical free energy reaction profile in the absence of the active site Mg^{2+}. Solid line represents the profile incorporating the electrostatic interactions with this Mg^{2+} estimated from *A*. The free energy reaction profiles are shown relative to P_{OH} for reasons described in the text. In the absence of Mg^{2+}, it is assumed that the tertiary interactions stabilizing S_A and P_{OH} are the same and therefore $E{\cdot}S_A + G$ and $E{\cdot}P_{OH} + GA$ are shown to be energetically equivalent. For clarity, the energetic barrier between $E{\cdot}S_A + G$ and the transition state is not drawn to scale.

40-fold weaker tertiary stabilization of S_A than P_{OH} on the ribozyme.‖‖ This result and the observation that the rates of the chemical step for CCCUCUpA analogs with different 2′ substituents on the U at the cleavage site have a dependence on the pK_a values of the leaving group similar to that observed for model phosphodiesters in solution (34) suggest that physical organic data in solution may provide estimates that apply reasonably well to the reaction in the ribozyme's active site.

CONCLUSIONS AND FURTHER IMPLICATIONS

It was previously suggested that tertiary interactions are important for preventing loss of the 5′ exon, which is analogous

¶¶The correlation in Fig. 3*A* is based on several estimations. A quantitative estimate has been provided to emphasize that substantial catalysis is predicted from these mechanisms, even though the values obtained are not precise—e.g., small differences in $\beta_{leaving\ group}$ values have been reported for different phosphodiester reactions (27, 34, 40, 41).

‖‖The similar values may be surprising considering that other favorable interactions of the phosphoryl group with E and environmental differences may mask the full destabilizing effect of placing a phosphorylated oxygen next to a Mg^{2+} (however, see text) (28, 29). If the interaction between the 3′ oxygen and Mg^{2+} were absent in the $E{\cdot}S_A$ ground state, the actual destabilization from a $Mg^{2+} \cdots$ (R)O-P interaction could be greater than the observed 40-fold. In this case, the destabilization mechanism could still operate, but with tertiary interactions insufficient to enforce the destabilizing $Mg^{2+} \cdots$ (R)O-P interaction in the ground state. Furthermore, the reaction $E{\cdot}S_A + G \rightarrow$ products is unaffected by 10–50 mM Mg^{2+} (unpublished results), suggesting that the Mg ions required for reaction are already bound in the $E{\cdot}S_A$ ground state. (See also ¶¶.)

to P_{OH}, following the first step of self-splicing (42). The subsequent finding that oligonucleotides bound in the P1 duplex dock into tertiary interactions with the catalytic core suggested that the ribozyme was also using tertiary interactions to align its substrates for reaction and to ensure cleavage at the correct phosphodiester bond (7–13, 19, 43). Furthermore, the weaker binding of a substrate having a 2′ OCH_3 group relative to a substrate with a 2′ H at a position three nucleotides 5′ of the cleavage site suggested a significant degree of local rigidity within this RNA active site (ref. 13; unpublished data).

The results presented here extend this view. The effective concentration of 2200 M for the 3′ OH group of the oligonucleotide substrate provides a quantitative indication that the ribozyme can utilize binding interactions away from the site of bond cleavage for precise positioning at the site of bond cleavage. This suggests that RNA enzymes, like protein enzymes can achieve significant rate enhancements by entropic fixation of substrates and catalytic groups (5).

The observed weaker tertiary stabilization of the oligonucleotide substrate relative to the product, combined with the previous identification of an active site Mg^{2+} (33), has also led to a model of electrostatic substrate destabilization. This is an example of the "Circe effect" described earlier for protein enzymes wherein the enzyme "entices" the substrate by strong attractive interactions away from the site of chemical transformation and positions it in an unfavorable environment that is better suited to stabilizing the transition state (5).

Previous work has indicated that GpA (Eq. **1**) binds ≈40-fold weaker than G (ref. 32; T.S.M., D.H., and T. R. Cech, unpublished data; R. Mei and D.H., unpublished data). The weaker binding could be due to destabilization of GpA on the ribozyme relative to G that results in a rate enhancement for the reverse reaction analogous to that described above for the forward reaction with S_A. The destabilization could arise from an interaction with a Mg ion, although as yet there is no direct evidence for the presence of a second Mg^{2+} in the active site.

Analogous destabilization is expected whenever a metal ion or hydrogen bond donor is positioned next to the bridge oxygen of a reactive phosphate group. Thus, substrate destabilization by a metal ion or hydrogen bond donor could be used more generally by RNA and protein enzymes catalyzing phosphodiester bond cleavage. The precursor tRNA substrate of the ribonuclease P ribozyme binds ≈30-fold weaker than the tRNA product, introducing the possibility of substrate destabilization (44). Substrate destabilization is a potential mechanism for protein enzymes such as the 3′-5′ exonuclease of DNA Pol I, DNase I, and alkaline phosphatase, which appear to have the reactive bridging oxygen positioned next to a metal ion that presumably stabilizes the oxyanionic leaving group in the transition state (45–47). Staphylococcal nuclease, ras GTPase protein, and fructose 1,6-bisphosphatase appear to have hydrogen bond donors in proximity of the reactive bridging oxygen that could provide analogous substrate destabilization and transition state stabilization (34, 48–50). The bridging oxygen of carbon esters also behaves as though it has a charge of +0.7 relative to a protonated oxygen (21) so that enzymes catalyzing carbon ester hydrolysis may use analogous substrate destabilization.

In summary, the results presented here extend a fundamental energetic concept of protein enzymes to RNA enzymes: the use of binding interactions away from the site of chemical transformation to facilitate the catalytic step. In addition, the results with the *Tetrahymena* ribozyme have suggested a mechanism for catalysis of phosphoryl transfer via substrate destabilization and transition state stabilization that accounts for 10^4-fold of the total 10^{11}-fold catalysis achieved by this RNA enzyme and may in part account for the catalysis of these reactions by protein enzymes.

We greatly appreciate a gift of the 5′ OH ribozyme from S. Strobel. We thank M. Khosla for technical assistance and S. Muthini (Clontech), A. Smith and E. Zuo (Protein and Nucleic Acid Facility, Stanford) and F. Wincott and A. DiRenzo (Ribozyme Pharmaceuticals) for oligonucleotide synthesis. This work was supported by National Institutes of Health Grant GM49243 to D.H. D.H. is a Lucille P. Markey Scholar in Biomedical Sciences and a Searle Scholar.

1. Kruger, K., Grabowski, P. J., Zaug, A. J., Sands, J., Gottschling, D. E. & Cech, T. R. (1982) *Cell* **31,** 147–157.
2. Altman, S. (1989) *Adv. Enzymol.* **62,** 1–36.
3. Cech, T. R. (1990) *Annu. Rev. Biochem.* **59,** 543–568.
4. Herschlag, D. & Cech, T. R. (1990) *Biochemistry* **29,** 10159–10171.
5. Jencks, W. P. (1975) *Adv. Enzymol.* **43,** 219–410.
6. Michel, F., Hanna, M., Green, R., Bartel, D. P. & Szostak, J. W. (1989) *Nature (London)* **342,** 391–395.
7. Pyle, A. M. & Cech, T. R. (1991) *Nature (London)* **350,** 628–631.
8. Bevilacqua, P. C. & Turner, D. H. (1991) *Biochemistry* **30,** 10632–10640.
9. Pyle, A. M., Murphy, F. L. & Cech, T. R. (1992) *Nature (London)* **358,** 123–128.
10. Herschlag, D., Eckstein, F. & Cech, T. R. (1993) *Biochemistry* **32,** 8299–8311.
11. Strobel, S. A. & Cech, T. R. (1993) *Biochemistry* **32,** 13593–13604.
12. Pyle, A. M., Moran, S., Strobel, S. A., Chapman, T., Turner, D. H. & Cech, T. R. (1994) *Biochemistry* **33,** 13856–13863.
13. Knitt, D. S., Narlikar, G. J. & Herschlag, D. (1994) *Biochemistry* **33,** 13864–13879.
14. Zaug, A. J., Grosshans, C. A. & Cech, T. R. (1988) *Biochemistry* **27,** 8924–8931.
15. Scaringe, S. A., Francklyn, C. & Usman, N. (1990) *Nucleic Acids Res.* **18,** 5433–5441.
16. Pon, R. T., Usman, N. & Ogilvie, K. (1988) *BioTechniques* **6,** 768–775.
17. Usman, N., Ogilvie, K. K., Jiang, M.-Y. & Cedergren, R. J. (1987) *J. Am. Chem. Soc.* **109,** 7845–7854.
18. McConnell, T. S., Cech, T. R. & Herschlag, D. (1993) *Proc. Natl. Acad. Sci. USA* **90,** 8362–8366.
19. Herschlag, D. (1992) *Biochemistry* **31,** 1386–1399.
20. Bevilacqua, P. C., Kierzek, R., Johnson, K. A. & Turner, D. H. (1992) *Science* **258,** 1355–1358.
21. Williams, A. (1992) *Adv. Phys. Org. Chem.* **27,** 1–55.
22. Lowry, T. H. & Richardson, K. S. (1987) *Mechanism and Theory in Organic Chemistry* (Harper and Row, New York), 3rd Ed., pp. 127–258.
23. Baes, C. F. J. & Mesmer, R. E. (1976) *The Hydrolysis of Cations* (Wiley, New York), pp. 95–98.
24. Jencks, W. P. & Regenstein, J. (1976) *Handbook of Biochemistry and Molecular Biology* (CRC, Cleveland, OH) p. 196–197.
25. Hudson, R. F. (1974) in *Chemical Reactivity and Reaction Paths*, ed. Klopman, G. (Wiley, New York), pp. 167–252.
26. Bourne, N. & Williams, A. (1980) *J. Org. Chem.* **49,** 1200–1204.
27. Khan, S. A., Kirby, A. J., Wakselman, M., Horning, D. P. & Lawlor, J. M. (1970) *J. Chem. Soc. B.*, 1182–1189.
28. Rajagopal, J., Doudna, J. A. & Szostak, J. W. (1989) *Science* **244,** 692–694.
29. Herschlag, D., Piccirilli, J. A. & Cech, T. R. (1991) *Biochemistry* **30,** 4844–4854.
30. Freier, S. M., Kierzek, R., Jaeger, J. A., Sugimoto, N., Caruthers, M., Nielson, T. & Turner, D. H. (1986) *Proc. Natl. Acad. Sci. USA* **83,** 9373–9377.
31. Bevilacqua, P. C., Li, Y. & Turner, D. H. (1994) *Biochemistry* **33,** 11340–11348.
32. Moran, S., Kierzek, R. & Turner, D. H. (1993) *Biochemistry* **32,** 5247–5256.
33. Piccirilli, J. A., Vyle, J. S., Caruthers, M. H. & Cech, T. R. (1993) *Nature (London)* **361,** 85–88.
34. Herschlag, D., Eckstein, F. & Cech, T. R. (1993) *Biochemistry* **32,** 8312–8321.
35. Thompson, R. C. (1974) *Biochemistry* **13,** 5495–5501.
36. Bode, W. (1979) *J. Mol. Biol.* **127,** 357–374.
37. Nakamura, C. E. & Abeles, R. H. (1985) *Biochemistry* **24,** 1364–1376.
38. Gilheany, D. G. (1992) in *The Chemistry of Organophosphorus Compounds*, ed. Hartley, F. R. (Wiley, New York), pp. 9–17.
39. Van Wazer, J. R. (1956) *J. Am. Chem. Soc.* **78,** 5709–5715.
40. Kirby, A. J. & Younas, M. (1970) *J. Chem. Soc. B.*, 1165–1172.
41. Steffens, J. J., Siewers, I. J. & Benkovic, S. J. (1975) *Biochemistry* **14,** 2431–2440.
42. Herschlag, D. & Cech, T. R. (1990) *Biochemistry* **29,** 10172–10180.
43. Strobel, S. A. & Cech, T. R. (1994) *Nat. Struct. Biol.* **1,** 13–17.
44. Beebe, J. A. & Fierke, C. A. (1994) *Biochemistry* **33,** 10294–10304.
45. Freemont, P. S., Friedman, J. M., Beese, L. S., Sanderson, M. R. & Steitz, T. A. (1988) *Proc. Natl. Acad. Sci. USA* **85,** 8924–8928.
46. Suck, D., Lahm, A. & Oefner, C. (1988) *Nature (London)* **321,** 620–625.
47. Kim, E. E. & Wyckoff, H. W. (1991) *J. Mol. Biol.* **218,** 449–464.
48. Cotton, F. A., Hazen, E. E. & Legg, M. J. (1979) *Proc. Natl. Acad. Sci. USA* **76,** 2551–2555.
49. Schlichting, I., Almo, S. C., Rapp, G., Wilson, K., Petratos, K., Lentfer, A., Wittinghofer, A., Kabsch, W., Pai, E. F., Petsko, G. A. & Goody, R. S. (1990) *Nature (London)* **345,** 309–315.
50. Zhang, Y., Liang, J., Huang, S., Ke, H. & Lipscomb, W. N. (1993) *Biochemistry* **32,** 1844–1857.